Synthesis, Spectroscopy, Crystal Structure, Electrochemistry, and Quantum Chemical and Molecular Dynamics Calculations of a 3-Anilino Difluoroboron Dipyrromethene Dye

Wenwu Qin,[†,‡] Volker Leen,[†] Taoufik Rohand,[†] Wim Dehaen,[†] Peter Dedecker,[†] Mark Van der Auweraer,[†] Koen Robeyns,[†] Luc Van Meervelt,[†] David Beljonne,[§] Bernard Van Averbeke,[§] John N. Clifford,[†] Kris Driesen,[†] Koen Binnemans,[†] and Noël Boens*[,†]

Department of Chemistry, Katholieke Universiteit Leuven, Celestijnenlaan 200f—bus 02404, 3001 Leuven, Belgium, College of Chemistry and Chemical Engineering, Lanzhou University, Lanzhou 730000, China, and Laboratory for Chemistry of Novel Materials, University of Mons-Hainaut, Place du Parc 20, 7000 Mons, Belgium

Received: September 1, 2008; Revised Manuscript Received: November 7, 2008

An asymmetrically substituted fluorescent difluoroboron dipyrromethene (BODIPY) dye, with a phenylamino group at the 3-position of the BODIPY chromophore, has been synthesized by nucleophilic substitution of 3,5-dichloro-8-(4-tolyl)-4,4-difluoro-4-bora-3a,4a-diaza-*s*-indacene. The solvent-dependent spectroscopic and photophysical properties have been investigated by means of UV−vis spectrophotometry and steady-state and time-resolved fluorometry and reflect the large effect of the anilino substituent on the fluorescence characteristics. The compound has a low fluorescence quantum yield in all but the apolar solvents cyclohexane, toluene, and chloroform. Its emission maxima in a series of solvents from cyclohexane to methanol are red-shifted by approximately 50 nm in comparison to classic BODIPY derivatives. Its oxidation potential in dichloromethane is at ca. 1.14 V versus Ag/AgCl. The absorption bandwidths and Stokes shifts are much larger than those of typical, symmetric difluoroboron dipyrromethene dyes. The values of the fluorescence rate constant are in the $(1.4-1.7) \times 10^8$ s^{-1} range and do not vary much between the solvents studied. X-ray diffraction analysis shows that the BODIPY core is planar. Molecular dynamics simulations show that there is no clear indication for aggregates in solution.

Introduction

Because of their favorable photophysical and optoelectronic properties, 4,4-difluoro-4-bora-3a,4a-diaza-*s*-indacene[1] (difluoro*bor*on *dipy*rromethene or BODIPY) derivatives have found widespread application as fluorescent labels in bioanalytics, as fluorophores in new chemosensors, or as laser dyes.[2−6] The excellent qualities of BODIPY comprise relatively high fluorescence quantum yields Φ_f (often approaching 1.0) and molar absorption coefficients (ε > 50 000 L mol^{-1} cm^{-1}), narrow emission bandwidths with high peak intensities, excellent thermal and photochemical stability, good solubility, chemical robustness, negligible triplet-state formation, and excitation/emission wavelengths in the visible region. Moreover, their building block synthesis allows one to develop many different BODIPY analogues with emission wavelengths tunable from 500 to over 700 nm, by attaching supplementary units at the pyrrole,[7] meso,[8−10] and N-ortho positions.[6,11−14] An interesting new class of BODIPY-related fluorophores is obtained by functionalization of the boron atom in the difluoroboradiaza-indacene unit via substitution of the F atoms with C- and O-centered groups.[2,15] The photophysical properties of several BODIPY dyes in solution have been studied by means of UV−vis absorption and fluorescence techniques.[10,16−18]

Although there are several positions on the BODIPY chromophore where functionalization can be carried out, suitable substituents at the 3- (and 5-) position(s) can shift the excitation and emission bands as a function of solvent polarity/polarizability. Recently, we described that the easily obtained 3,5-dichloro-4,4-difluoro-4-bora-3a,4a-diaza-*s*-indacene derivatives[19] can be substituted with a wide range of oxygen-, carbon-, nitrogen-, and sulfur-centered nucleophiles[6,11] and that the reaction conditions can be adjusted to have either mono or disubstitution.[11] The solvent-dependent photophysical characteristics of four BODIPY derivatives with uncommon substituents such as chloro, methoxy, and malonate at the 3,5-positions were investigated by means of UV−vis spectrophotometry and steady-state and time-resolved fluorometry.[20] Their absorption (from 508 to 517 nm) and emission (from 519 to 530 nm) maxima are very similar to those of conventional BODIPY dyes, showing small Stokes shifts (between 440 and 490 cm^{-1}) and narrow absorption (full width at half-maximum, $fwhm_{abs}$, between 710 and 820 cm^{-1}) and emission bands.

Some work has been done toward developing BODIPY derivatives with absorption and emission spectra shifted to longer wavelengths by increasing the conjugation at the 3,5-positions.[4,5,18,21,22] In the present work, we describe the detailed procedure for the synthesis of a 3-anilino-5-chloro substituted BODIPY dye (**2**) via the recently described substitution reaction[11] of 3,5-dichloro-8-(4-tolyl)-4,4-difluoro-4-bora-3a,4a-diaza-*s*-indacene (**1**) with aniline as nucleophile. In addition, we investigate the spectroscopic and photophysical characteristics of **2** in several solvents by UV−vis absorption spectrophotometry and steady-state and time-resolved fluorescence spectroscopy. From these experiments we could determine the wavelengths of the spectral maxima [λ_{abs}(max), λ_{ex}(max), λ_{em}(max)], the full width at half-maximum of the absorption band ($fwhm_{abs}$, in cm^{-1}), the full width at half-maximum of the fluorescence emission band ($fwhm_{em}$, in cm^{-1}), the Stokes shifts

* To whom correspondence should be addressed. E-mail: Noel.Boens@chem.kuleuven.be.
† Katholieke Universiteit Leuven.
‡ Lanzhou University.
§ University of Mons-Hainaut.

10.1021/jp8077584 CCC: $40.75
Published on Web 12/19/2008

SCHEME 1: Synthesis of the BODIPY Derivative 2[a]

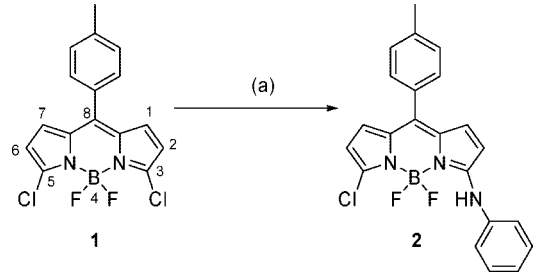

[a] Reaction conditions: (a) rt/aniline/CH_3CN/14 h.

($\Delta\bar{\nu}$, in cm^{-1}), the fluorescence quantum yields (Φ_f) and lifetimes (τ), and the rate constants of fluorescence (k_f) and nonradiative (k_{nr}) deactivation. Next, the electrochemical properties of **2** have been measured, and furthermore, its crystallographic structure has been determined. Finally, quantum chemical and molecular dynamics calculations have been applied to elucidate the UV−vis absorption spectra of **2**.

Experimental Section

Materials. All solvents for the spectroscopic measurements were of spectroscopic grade and were used without further purification. The chemicals for the synthesis were of reagent grade quality, procured from commercial sources, and used as received.

Synthesis.

3,5-Dichloro-8-(4-tolyl)-4,4-difluoro-4-bora-3a,4a-diaza-s-indacene (1)[20] is the starting compound for the synthesis of BODIPY derivative **2** (Scheme 1).

5-Chloro-3-phenylamino-8-(4-tolyl)-4,4-difluoro-4-bora-3a,4a-diaza-s-indacene (2). To a stirred solution of **1** (100 mg, 0.29 mmol) in acetonitrile (50 mL) under nitrogen atmosphere was added aniline (104 μL, 1.20 mmol). The reaction mixture was stirred at room temperature for 14 h. Then the reaction mixture was poured in water, and the product was extracted with dichloromethane (2 × 50 mL). The combined extracts were washed with water and brine, dried over $MgSO_4$, and evaporated to dryness under reduced pressure. The solid residue was chromatographed on silica gel with heptane/dichloromethane 7:3 (v/v) as eluent to yield 81 mg (69% yield) of brick-red crystals. Mp 183 °C. ^{1}H NMR ($CDCl_3$) δ 8.10 (s, broad, NH), 7.44−7.33 [m, 4H (tolyl)], 7.28−7.24 [m, 5H (Ph)], 6.93 [d, 1H (H-6), J = 4.6 Hz), 6.44 [d, 1H (H-1), J = 3.7 Hz], 6.42 [d, 1H (H-7), J = 4.6 Hz], 6.23 [d, 1H (H-2), J = 3.7 Hz], 2.44 [s, 3H, CH_3 (tolyl)]; ^{13}C NMR ($CDCl_3$) δ 159.1 (s), 140.0 (s), 137.7 (d), 135.9 (s), 134.3 (s), 132.4 (s), 131.6 (s), 130.6 (d), 129.4 (d), 126.5 (d), 122.9 (d), 122.1 (s), 113.7 (d), 111.9 (d), 20.9 [q, CH_3 (tolyl)]; LRMS (EI, 70 eV) m/z 407 (M^+ 100), 409 (M^+ 31); HRMS: calcd for $C_{22}H_{17}BClF_2N_3$ 407.1172, found 407.1191.

^{1}H and ^{13}C NMR spectra were recorded at room temperature on a Bruker Avance 300 instrument operating at a frequency of 300 MHz for ^{1}H and 75 MHz for ^{13}C. ^{1}H NMR spectra were referenced to tetramethylsilane (0.00 ppm) as an internal standard. Chemical shift multiplicities are reported as s = singlet, d = doublet, q = quartet, and m = multiplet. ^{13}C NMR spectra were referenced to the $CDCl_3$ (77.67 ppm) signal. Mass spectra were recorded on a Hewlett-Packard 5989A mass spectrometer (EI mode and CI mode). High-resolution mass data were obtained with a Kratos MS50TC instrument. Melting points were taken on a Reichert Thermovar and are uncorrected.

Crystal Structure Determination. Compound **2** was crystallized from cyclohexane/chloroform (9:1, v/v), yielding red crystals with an average size of 0.2 × 0.1 × 0.05 mm^3. The crystals belonged to the monoclinic space group $P2_1/n$ (number 14) with cell dimensions a = 12.134(8) Å, b = 12.926(8) Å, c = 12.543(7) Å, β = 107.85(2)°, V = 1873(2) $Å^3$, Z = 4, ρ_{calc} = 1.446 g cm^{-3}, $2\theta_{max}$ = 142.2°, μ(Cu Kα) = 2.090 cm^{-1}. The data were measured on a Bruker SMART 6000 detector, Cu Kα (λ = 1.54178 Å) with crossed Göbel mirrors. The crystals were cryocooled to 100 K. A total of 18 737 reflections were measured of which 3559 are unique reflections. The data were corrected for Lorentz, absorption (Bruker SADABS), and polarization effects. The structure was solved by direct methods. Full-matrix least-squares refinement based on F^2 (SHELXL97),[23] 277 parameters, with hydrogen atoms placed at calculated positions with temperature factors 20% higher than parent atom and the hydrogen bond distances free to refine resulted in R_1 = 0.0428 [for 2946 with $I > 4\sigma(I)$], ωR_2 = 0.1052, max/min residual electron density 0.30/−0.24 e^- $Å^{-3}$.

Crystallographic data (excluding structure factors) for the structure reported in this paper have been deposited with the Cambridge Crystallographic Data Centre as supplementary publication no. CCDC−622572. Copies of the data can be obtained free of charge on application to CCDC, 12 Union Road, Cambridge CB2 1EZ, U.K. (fax: +44(0)-1223-336033 or e-mail: deposit@ccdc.cam.ac.uk).

Cyclic Voltammetry. Electrochemical data were obtained using an Autolab PGSTAT12 potentiostat and a standard three-electrode cell (platinum working and counter electrodes and an Ag/AgCl reference) at a scan rate of 200 mV s^{-1}. The voltammograms were recorded at room temperature in a solution of 0.1 mol L^{-1} tetrabutylammonium hexafluorophosphate as the supporting electrolyte in dry dichloromethane. All solutions were purged with argon prior to measurement.

UV−Vis Steady-State Spectroscopy. UV−vis absorption spectra were recorded on a Perkin-Elmer Lambda 40 UV−vis spectrophotometer, whereas for the corrected steady-state excitation and emission spectra, a SPEX Fluorolog was employed. All absorption and fluorescence excitation/emission spectra were recorded at 20 °C using nondegassed samples (degassing did not influence the fluorescence quantum yield). For the dye in a specific solvent, three or four absorption, excitation, and emission spectra were measured as a function of dye concentration. Since the spectra are recorded digitally and the peaks are relatively narrow, the maxima can be determined not only from visual inspection but also via the analysis−calculus−integrate menu of the Origin software. The error on the wavelength of the maximum is usually 1−2 nm. For the determination of the relative fluorescence quantum yields (Φ_f), only dilute solutions with an absorbance below 0.1 at the excitation wavelength λ_{ex} were used. Rhodamine 6G in H_2O (λ_{ex} = 488 nm, Φ_f = 0.76) was used as fluorescence standard.[24] The Φ_f values reported in this work are the averages of multiple (generally three or four), fully independent measurements. The majority of the Φ_f determinations was done on nondegassed samples. To check the influence of dissolved O_2 on Φ_f, a few samples, degassed via successive freeze−pump−thaw cycles, were measured. The obtained Φ_f values were within experimental error equal for aerated and degassed samples, in accordance with results for other BODIPY compounds.[10a] In all Φ_f determinations, correction for the solvent refractive index was applied.[25]

Time-Resolved Fluorescence Spectroscopy. Fluorescence decay traces of BODIPY derivative **2** were recorded at several emission wavelengths by the single-photon timing method.[26]

Details of the instrumentation used and experimental procedures have been described elsewhere.[27] The samples were excited at 488 nm with a repetition rate of 8.10 MHz, using the frequency-doubled output from an OPO pumped by a picosecond Ti: Sapphire laser. Fluorescence decay histograms were collected at magic angle in 4096 channels with a time increment per channel of 1.8 ps, using 10 × 10 mm^2 optical path length cuvettes. The absorbance at the excitation wavelength was always below 0.1. All lifetime measurements were performed on samples that were degassed by consecutive freeze−pump−thaw cycles. This is common practice in our laboratory because we want to guarantee excluding the effect of dissolved oxygen on the fluorescence lifetimes. After analysis of the initial fluorescence decay curves indicates that degassing is not necessary, we usually start collecting the remaining fluorescence decay traces using nondegassed samples. The fluorescence lifetime of **2** in the three solvents used did not change upon degassing. Histograms of the instrument response function were recorded using a LUDOX scatterer. The fwhm of the instrument response function was ~60 ps. All measurements were done at 20 °C.

The fitting parameters were determined by minimizing the global, *reduced* chi-square χ_g^2:

$$\chi_g^2 = \sum_l^q \sum_i w_{li}(y_{li}^o - y_{li}^c)^2/\nu \quad (1)$$

where the index l sums over q experiments, and the index i sums over the appropriate channel limits for each individual experiment. y_{li}^o and y_{li}^c denote, respectively, the observed and calculated (i.e., fitted) values corresponding to the ith channel of the lth experiment, and w_{li} is the corresponding statistical weight. ν represents the number of degrees of freedom for the entire multidimensional fluorescence decay surface.

The statistical criteria for assessing the quality of the fit included both graphical and numerical tests and have been described elsewhere.[26c,28] Decays were analyzed first individually by a (multi)exponential decay law in terms of decay times τ_i and their associated pre-exponential factors α_i. The final curve-fitting was done by global analysis in which decays recorded at six different emission wavelengths λ_{em} (550, 560, 570, 600, 620, and 650 nm) were described by a single-exponential decay function with linked lifetime τ and local (nonlinked) pre-exponentials α. The quality of the fit was judged for each fluorescence decay trace separately as well as for the global fluorescence decay surface. All curve-fittings presented here had χ^2 values below 1.1.

For the single-exponential fluorescence decays, the rate constants of fluorescence (k_f) and nonradiative (k_{nr}) deactivation can be calculated from the measured fluorescence quantum yield Φ_f and lifetime τ according to eqs 2 and 3:

$$k_f = \Phi_f/\tau \quad (2)$$

$$k_{nr} = (1 - \Phi_f)/\tau \quad (3)$$

Computational Details. Molecular properties in the gas phase were obtained using semiempirical and ab initio quantum chemical methods. The ground-state (respectively, excited-state) geometries of compound **2** were computed at the AM1 (respectively, AM1/CI)[29] and DFT/B3LYP[30] levels. These structures were subsequently used as input for electronic excited-state calculations performed at the INDO/SCI level.[31] The highest 30 occupied and 30 unoccupied molecular orbitals were included in the SCI active space. Conformational fluctuations and their impact on the spectroscopic properties were also accounted for through molecular dynamics (MD) simulations of one BODIPY molecule embedded in a solvent box (in our simulations we used tetrahydrofuran, THF), using the DREIDING force field.[32] MD simulations were run for a period of 100 ps within the canonical ensemble (using fixed temperature, pressure, and number of particles) at room temperature. A total of 30 snapshots were extracted from the MD trajectory and considered further for INDO/SCI excited-state calculations. We also took into account the possible formation of small aggregates in solution. To do so, the same MD and INDO/SCI simulations were performed for two molecules (facing each other in the initial configuration) in the solvent bath.

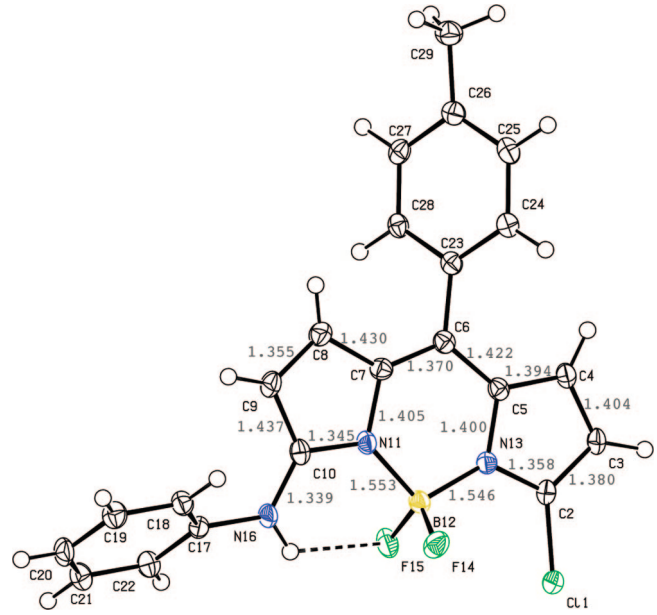

Figure 1. PLATON/Ortep (Spek, A. L. *J. Appl. Crystallogr.* **2003**, *36*, 7−13) representation of compound **2** with displacement ellipsoids at the 50% probability level. The intramolecular hydrogen bond between the NH group and the fluorine atom is indicated by a dashed line, and the BODIPY bond lengths are shown in gray.

Results and Discussion

Compound **2** was synthesized by an efficient nucleophilic substitution reaction of compound **1**.[6,11] This synthetic methodology is extremely useful for obtaining nonsymmetrically and symmetrically substituted boradiazaindacene dyes with substituents at the 3- (and 5-) position(s) that are difficult to realize otherwise. The crystal structure of **2** has been determined, and its photophysical properties in various solvents and its electrochemical properties in dichloromethane have been investigated.

Crystallographic Structure. In compound **2** (Figure 1), the BODIPY ring system is flat (max deviation 0.051 Å for boron atom), with the two fluorine atoms above and under the plane. This is in contrast with the majority of BODIPY structures found in the Cambridge Structural Database (CSD)[33] where the angle between the two pyrrole moieties is on average 5.4° (range 0−18°) and where a maximum displacement of 0.34 Å from the BODIPY plane is observed for the boron atom. The phenyl ring at the meso position makes an angle of 54.8° with the BODIPY core, which is in the range of most BODIPY derivatives (40.3−90°), but is smaller than the average value of 74.5° found in the CSD.

At least one intramolecular hydrogen bond is found between the NH group and one of the fluorine atoms; the interaction with the second fluorine atom is probably weak or absent

[$d(N_{16}H_{16}) = 0.86$ Å, $d(H_{16}\cdots F_{15}) = 2.43$ Å, ang($N_{16}H_{16}\cdots F_{15}$) = 124.3°, $d(H_{16}\cdots F_{14}) = 2.77$ Å, ang($N_{16}H_{16}\cdots F_{14}$) = 112.4°]. The nonsymmetric substitution pattern is reflected in the pyrrole bond distances.

Electrochemistry. The oxidation potential of **2** estimated from the midpoints of the forward and reverse peaks of the scan in the cyclic voltammogram appears at ca. 1.14 V versus Ag/AgCl. Upon scanning in the cathodic direction, a precipitate can be clearly seen to form on the surface of the working electrode, which could be due to instability of the oxidized form of **2**. This observation manifests itself with the reverse scans displaying smaller current amplitudes than the forward scans. Upon moving to faster scan rates this effect appears less pronounced; however, fully reversible forward and reverse scans are still not observed. We did not observe any reduction electrochemistry for **2**, and this could be because the redox potential is beyond the accessible range of dichloromethane. Even extending this range in the cathodic direction using solvents as THF and acetonitrile did not lead to the observation of a reduction wave.

Spectroscopic Properties. Figure 2a shows the absorption and steady-state fluorescence emission spectra of **2** in cyclohexane. The absorption spectrum is of comparable shape as those of described BODIPY dyes,[10,16−20,34] with an intense absorption band somewhat above 500 nm and a less pronounced shoulder at shorter wavelengths. The absorption spectra of **2** in other solvents (Figure 2b) are analogous to that in cyclohexane, and they all show two absorption bands: (1) in the visible wavelength region, the 0−0 band of a strong S_0-S_1 transition with a maximum ranging from 498 to 529 nm (Table 1) and a (more or less pronounced) shoulder on the high-energy side, which is attributed to the 0−1 vibrational band of the same transition. The wavelengths of these absorption maxima λ_{abs}(max) (Table 1) are very similar to those of other typical BODIPY derivatives.[10,16,17,20,34] The absorption spectra are dependent on solvent polarity; the maximum being blue-shifted (by ∼30 nm) when the solvent is changed from cyclohexane (529 nm) to methanol (498 nm). (2) Additionally, a weaker, broad absorption band is found in the UV at about 350 nm, the position of which is not appreciably affected by solvent polarity. This broader and weaker absorption band is attributed to the S_0-S_2 transition. The $fwhm_{abs}$ of the intense absorption band around 500 nm is in the 2500−3500 cm^{-1} range (Table 1), which is significantly more than generally found for BODIPY derivatives substituted at the 3- and 5-positions by weaker electron donors or electron-withdrawing groups (e.g., $fwhm_{abs}$ for **1** is in the 650−780 cm^{-1} range).[20] One should note that already in an apolar solvent as cyclohexane the $fwhm_{abs}$ is already several times larger than that observed for other common BODIPY derivatives. This indicates that upon excitation a significant change in bond lengths or angles occurs.

Compound **2** in cyclohexane shows an emission spectrum with a maximum at 567 nm, shaped like the mirror image of the absorption spectrum, displaying the typical emission features of boron dipyrromethene.[10,16,17,20,34] Besides the 0−0 transition at 567 nm, there is the 0−1 transition, visible as a shoulder peak located at 615 nm. The difference (1380 cm^{-1}) matches the frequency of a conjugated double bond. This is to be expected because small changes in bond length of the different bonds in the conjugated system can occur upon excitation. The maximum wavelength of the fluorescence band is hardly affected by solvent polarity (Figure 2c, Table 1): there is only a 9 nm difference between the wavelengths of the emission maxima λ_{em}(max) in toluene (575 nm) and methanol (566 nm). In more polar solvents the broadening of the individual vibronic bands due to solvent interactions blurs out the vibrational progression observed in cyclohexane. The wavelength of the emission maximum of **2** is red-shifted by ∼50 nm compared to other described BODIPY dyes[10,16,17,34] (e.g., λ_{em}(max) for **1** varies between 529 nm in toluene and 519 nm in methanol).[20] The $fwhm_{em}$ varies between 1815 cm^{-1} in cyclohexane and 2384 cm^{-1} in THF (Table 1). There is an excellent parallel between the corresponding values of $fwhm_{abs}$ and $fwhm_{em}$ for each solvent. The best linear fit of $fwhm_{em}$ (y-values) as a function

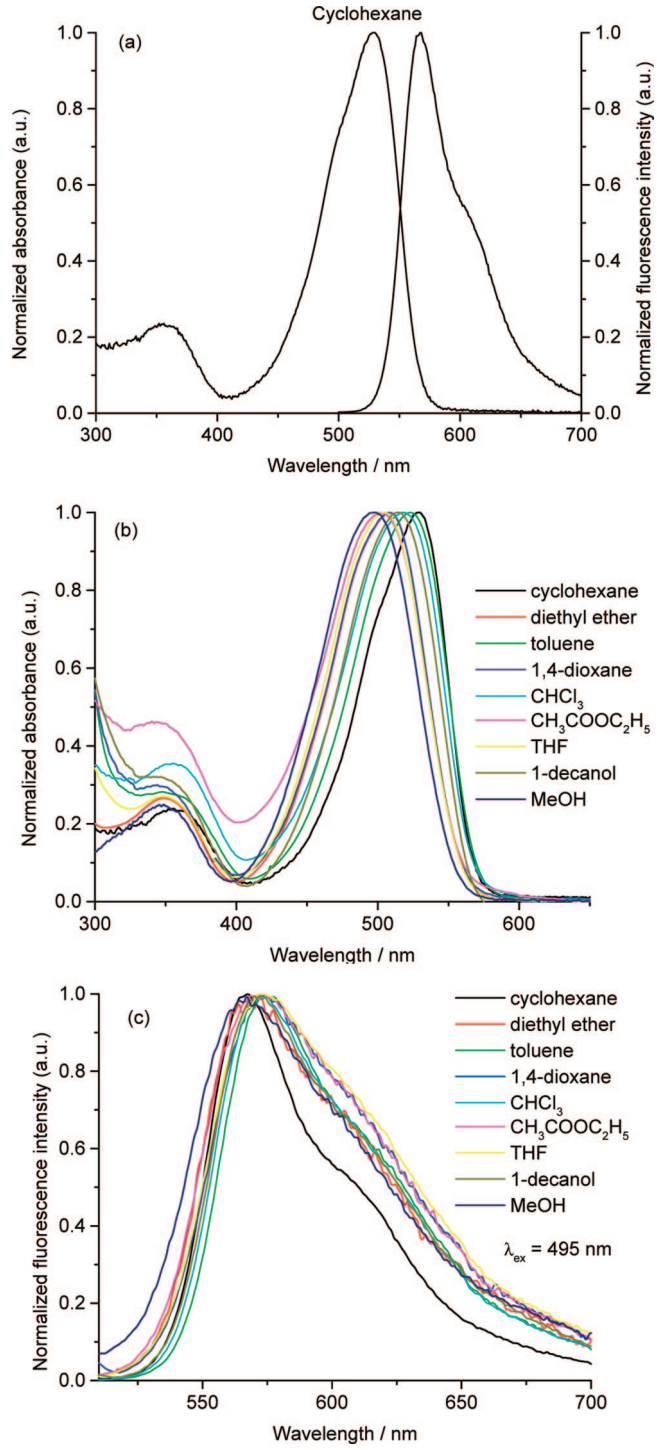

Figure 2. (a) Absorption and fluorescence emission spectra of **2** in cyclohexane normalized to 1.0. (b) Analogously normalized absorption spectra of **2** in different solvents. (c) Corresponding normalized fluorescence emission spectra (excitation at 495 nm).

TABLE 1: Photophysical Data of Dye 2 in Several Solvents

	solvent[a]	λ_{abs}(max)/nm	λ_{em}(max)/nm	λ_{ex}(max)/nm	fwhm$_{abs}$/cm^{-1}	fwhm$_{em}$/cm^{-1}	$\Delta\bar{\nu}$/cm^{-1}	Φ_f	τ/ns[b]	$k_f/10^8$ s^{-1}	$k_{nr}/10^8$ s^{-1}
1	cyclohexane	529	567	529	2545	1815	1267	0.28	1.96	1.4	3.7
2	1,4-dioxane	508	573	508	3199	2334	2233	0.026			
3	toluene	524	575	524	2860	2094	1693	0.35	2.03	1.7	3.2
4	diethyl ether	509	570	509	3105	2308	2103	0.008			
5	chloroform	519	572	519	2983	2109	1785	0.26	1.62	1.6	4.6
6	ethyl acetate	504	572	504	3453	2375	2359	0.01			
7	THF	505	574	505	3212	2384	2380	0.008			
8	1-decanol	514	570	514	3098	2200	1911	0.044			
9	methanol	498	566	498	3292	2365	2412	0.003			

[a] The solvents are classified according to increasing polarity (as measured by the dielectric constant ε). [b] The standard errors on all lifetimes τ are $\leq$10 ps.

of fwhm$_{abs}$ (x-values) gives $y = 126 + 0.679x$ (in cm^{-1}) with a correlation coefficient of 0.952. When compared to other, classic BODIPY derivaties,[10,16−18] **2** shows a much larger fwhm in both absorption and emission and a considerable larger Stokes shift of the 0−0 vibronic transition. This indicates that along a coordinate with a small force constant (torsions and/or solvation) and hence with a separation of vibrational levels ($h\nu_{vib}$) smaller than kT, there is a significant shift between the minima of the potential energy surfaces in the ground state and the excited state.[35] When only low-frequency vibrations ($h\nu_{vib} < kT$) are considered, the Stokes shift, $\Delta\bar{\nu}$, and bandwidth, fwhm (all in cm^{-1}), are proportional to λ, the reorganization energy, and $\sqrt{\lambda}$, respectively. Indeed, the Stokes shift is equal to $\Delta\bar{\nu} = 2\lambda$, whereas the bandwidth amounts to fwmh $= 4((\ln 2)\,\lambda\,kT)^{1/2}$. Substitution of λ, obtained from the experimental Stokes shift, in the formula for fwhm always underestimates fwhm. The larger value of the experimental fwhm is due to the 0−1 vibronic transition of a high-frequency vibration in the spectrum. This relation also explains why the Stokes shift and fwhm evolve in parallel upon increasing the solvent polarity.

Contrary to the near-invariance of the emission wavelength maximum λ_{em}(max) in different solvents, the fluorescence quantum yield Φ_f of **2** is strongly solvent-dependent. The Φ_f values are moderately high in cyclohexane (0.28), toluene (0.35), and chloroform (0.26), whereas in all other solvents used the emission intensity is strongly quenched ($\Phi_f < 0.044$). Similar solvent-dependent Φ_f changes have been observed for BODIPY analogues with a 4-*N*,*N*-dimethylaminophenyl substituent at the meso position.[10,17] But unlike for these latter compounds, no red-shifted, broad, and solvent polarity-dependent fluorescence band originating from an intramolecular charge-transfer state (ICT) was found in the emission spectrum of **2**. Indeed, there is no direct spectral indication for two separate emission bands (from the locally excited state and an ICT state) in the emission spectra of **2**. The Stokes shift $\Delta\bar{\nu} = \bar{\nu}_{abs} - \bar{\nu}_{em}$ [with $\bar{\nu}_{abs}$ and $\bar{\nu}_{em}$ corresponding to the wavelengths λ_{abs}(max) and λ_{em}(max), respectively] increases nearly 2-fold between cyclohexane (1267 cm^{-1}) and methanol (2412 cm^{-1}) and is significantly larger than the Stokes shifts observed for 3,5-dichloro-BODIPY **1** (440 $\pm$ 30 cm^{-1}).[20] This agrees with the increased electron phonon coupling suggested by the fwhm$_{abs}$ of **2** in cyclohexane. This can perfectly be understood in the framework developed for cyanine dyes.[36] For symmetric BODIPYs there are two equivalently contributing Lewis structural formulas, and all bonds along the conjugated chain have a similar length which only increases slightly and homogeneously upon excitation. For **2**, however, the two delocalized structures A and B (Figure 3) are not equivalent any longer, with structure B being more stable. Moreover, one can write one extra stable, delocalized, Lewis structural formula (C in Figure 3) in which the anilino nitrogen

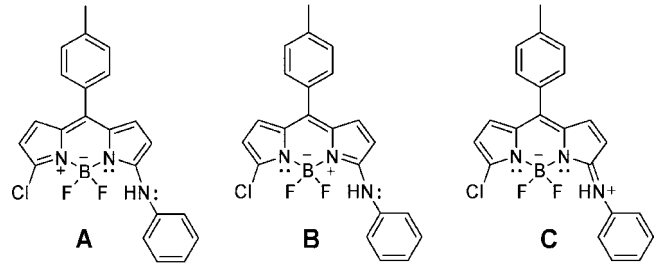

Figure 3. Major Lewis structural formulas contributing to the real structure of compound **2**.

TABLE 2: Spectroscopic Properties of Compound 2 in the Gas Phase[a]

	λ_{abs}(max)/nm	λ_{em}(max)/nm
AM1//INDO/SCI	504	533
DFT(B3LYP)//INDO/SCI	503	

[a] Compare these spectroscopic data with the experimental ones in solvents (Table 1).

donates a lone electron pair to the conjugated chain. As a consequence bond alternation starts to occur in the ground state, and this alternation will be inverted upon excitation, leading to increased electron phonon coupling. Also the solvent dependence of Φ_f and $\Delta\bar{\nu}$ may be interpreted as indication of a small contribution of a dipolar resonance form to the ground or excited state of **2**. The blue shift of the absorption spectrum from cyclohexane to THF or ethyl acetate can hardly be attributed to a difference in solvent polarizability. If it is attributed to dipolar interactions, this blue shift suggests that the dipole moment of the ground state is larger than that of the excited state, as supported by the quantum chemical calculations, vide infra. The latter also explains why the increased Stokes shift in methanol (compared to cyclohexane) is related to a blue shift of the absorption rather than to a red shift of the emission spectrum. This would suggest that the increase of the electron density in the conjugated BODIPY system by the anilino moiety is less outspoken in the excited state than in the ground state.

Plots of the maxima of absorption ($\bar{\nu}_{abs}$) and emission ($\bar{\nu}_{em}$) of **2** in all solvents versus $f(n^2) = (n^2 - 1)/(2n^2 + 1)$ (Figure S1, Supporting Information) indicate an inadequate linear relationship (correlation coefficient $r = -0.784$ for $\bar{\nu}_{abs}$ and $r = -0.657$ for $\bar{\nu}_{em}$). A similar poor relationship ($r = 0.687$, Figure S2, Supporting Information) was found for the Stokes shift $\Delta\bar{\nu}$ of **2** in all solvents versus the Lippert solvent parameter $\Delta f = f(\varepsilon) - f(n^2) = [(\varepsilon - 1)/(2\varepsilon + 1)] - [(n^2 - 1)/(2n^2 + 1)]$.[37,38] The relationship between the Stokes $\Delta\bar{\nu}$ of **2** and Δf is equally poor for the aprotic solvents only ($r = 0.620$). The reason is probably that although shifts induced by solvent polarity and solvent polarizability are of the same magnitude

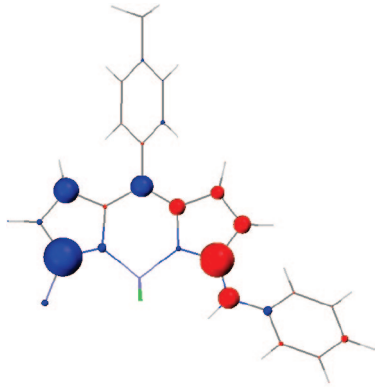

Figure 4. Transition density distribution calculated at the INDO/SCI level for the first optical transition of compound **2**. The blue spheres depict the negative charges, whereas red spheres indicate the presence of a positive charge.

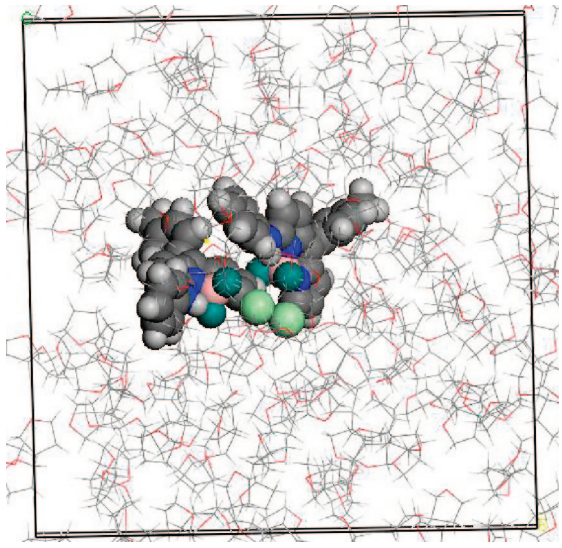

Figure 5. Snapshot at 30 ps of a molecular dynamics run for compound **2** in THF.

in **2**, those properties do not vary in a parallel way over the series of solvents used. In this way **2** differs significantly from most typical BODIPYs where the absorption ($\bar{\nu}_{abs}$) and emission ($\bar{\nu}_{em}$) maxima shift to lower energy linearly with increasing $f(n^2)$ while the Stokes shift is nearly independent of solvent polarity. Hence, in contrast to these BODIPYs the charge density on the conjugated chain of **2** changes upon excitation. The blue shift from cyclohexane over diethyl ether to methanol clearly suggests a larger dipole moment in the ground state compared to the excited state. This is also supported by the quantum chemical calculations, vide infra.

To investigate the fluorescence dynamics of **2**, fluorescence decay traces in cyclohexane, toluene, and chloroform were collected as a function of emission wavelength. All fluorescence decay profiles of **2** could be described by a single-exponential fit in the solvents used. The lifetimes τ estimated via single curve analysis were independent of the observation wavelength. Simultaneous (or global) curve-fitting of the fluorescence decay surface with τ linked as a function of the observation wavelength confirmed that the decays are indeed single-exponential and do not depend on the emission wavelength. The estimated fluorescence lifetimes τ are compiled in Table 1.

Using the experimental Φ_f and τ values, one can calculate (according to eqs 2 and 3) values for the rate constants of radiative (k_f) and radiationless (k_{nr}) decay. The values of k_f are in the $(1.4-1.7) \times 10^8$ s^{-1} range for the three investigated solvents (cyclohexane, toluene, and chloroform), indicating that k_f is nearly independent of the low-polarity solvent used. However, the absence of lifetime data in more polar solvents (due to the very low Φ_f values) makes it difficult to determine the trend of k_f and k_{nr} in more polar solvents. The k_f values obtained for **2** are very comparable to those obtained for compound **1** (k_f between 1.4×10^8 and 1.8×10^8 s^{-1}).[20] As before,[10,20] the largest k_f value is found in toluene. The k_{nr} values as a function of solvent are in the $(3.2-4.6) \times 10^8$ s^{-1} range, comparable to what was found before for BODIPY derivatives.[10,16−18,20]

Quantum Chemical and Molecular Dynamics Calculations. The existence of ground-state dimers of a few BODIPY analogues, especially in molecularly confined environments, has been reported.[39] Using quantum chemical and MD calculations, we want to investigate if evidence for ground-state dimers of dye **2** can be uncovered.

Molecule 2 in the Gas Phase. The spectroscopic properties (absorption and emission vertical transition energies) calculated at INDO/SCI level for both AM1 and DFT(B3LYP) optimized structures of compound **2** in the gas phase are compiled in Table 2 and should be compared to the experimental ones in solvents (reported in Table 1).

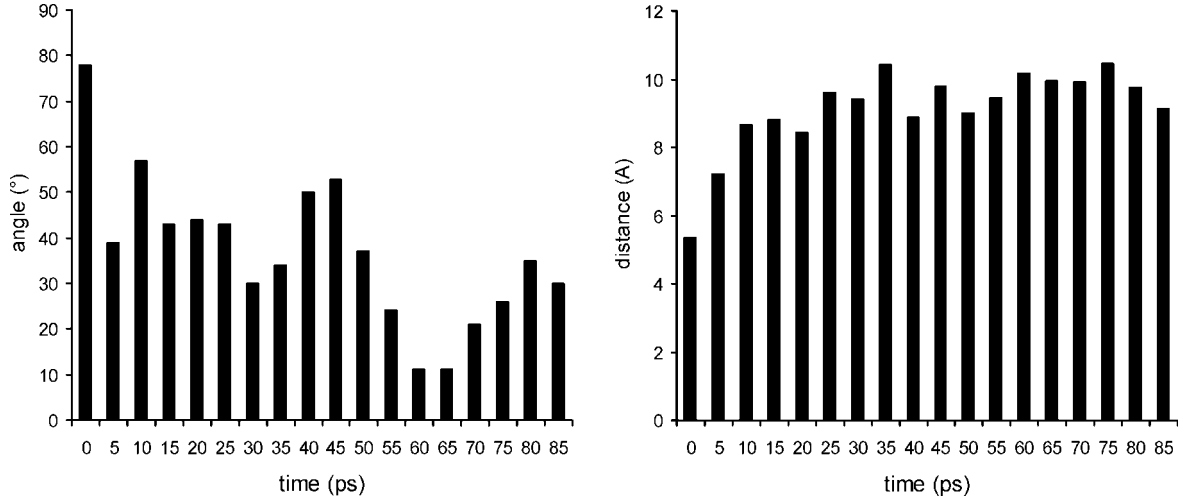

Figure 6. Angle, β, between the molecular plane and the intermolecular axis passing through the geometric centers (left) and center-to-center distance (right), as followed along an MD run performed for two molecules **2** embedded in a THF box.

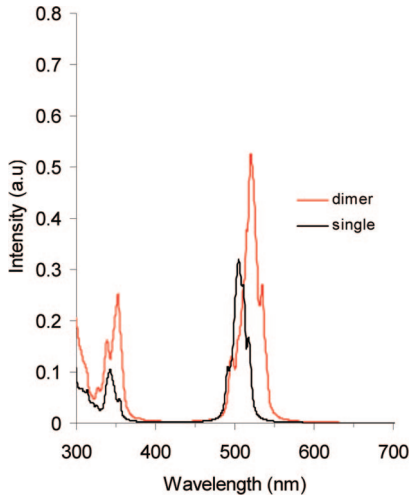

Figure 7. INDO/SCI absorption spectra of a single molecule and a dimer of compound **2** in THF. Ensemble spectra are averaged over 30 snapshots.

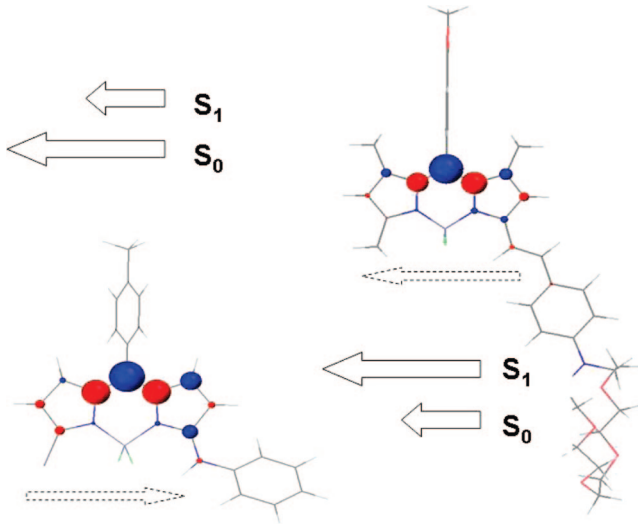

Figure 8. INDO/SCI (ZDO) changes in atomic charge density when going from the ground state to the lowest electronic excited state of **2** (left). For comparison, the corresponding charge redistribution is shown for compound **3** (right). Red circles correspond to positive partial charges, and blue circles correspond to negative charges. The solid line arrows represent the ground-state (S_0) and excited-state (S_1) dipole moment; the dotted arrows show the dipole moment difference.

The quantum chemical calculations reproduce qualitatively the overall trends observed experimentally. The transition density distribution for the first optical transition of compound **2** is depicted in Figure 4. The calculations underestimate the Stokes shift, which might be due to solvent effects not accounted for at this stage.

Molecule 2 in a Solvent Box. A snapshot of two molecules **2** embedded in a THF bath is shown in Figure 5.

The simulations show that, starting from a closely spaced, cofacial-like arrangement, the two molecules tend to separate from each other, which we associate mostly to electrostatic repulsion between the chlorine and fluorine atoms bearing larger negative charges. This can be clearly seen by following along the MD run the geometric center-to-center distance as well as the angle, β, between the molecular plane and the intermolecular axis passing through the molecular centers (see Figure 6).

The time evolution of the structural parameters suggests a sliding of one molecular plane with respect to the second one

TABLE 3: INDO/SCI State Dipole Moments (in debye, D) in the Ground State (S_0) and Excited State (S_1) of 2 and 3[a]

	2/D	**3**/D
S_0	8.76	6.47
S_1	5.65 (5.84)	8.30 (8.95)

[a] The numbers in between parentheses are the dipoles calculated for the relaxed excited-state geometry.

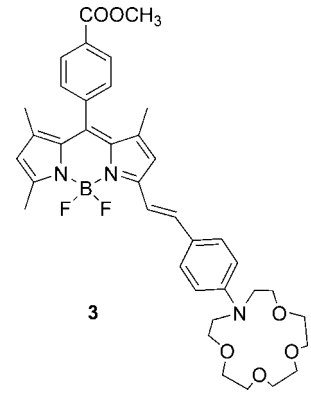

Figure 9. Structure of BODIPY dye **3**.

(consistent with a decrease of β from ~90° to ~30°) accompanied by an increased center-to-center separation (from ~5 to ~9 Å), as time goes by. It is also worth noting that these geometrical parameters fluctuate significantly in time, likely because of the nonplanar conformation of the molecules (the anilino group is out of the plane formed by the BODIPY core). Thus, the MD simulations suggest that aggregates of **2** are very unlikely in THF at room temperature. Yet, to check the effect of intermolecular interactions, the absorption spectra have been computed for both a single molecule and a dimer of **2** in THF. The ensemble (averaged over 30 snapshots) spectra displayed in Figure 7 are consistent with the structural analysis above. Except for a slight red shift (due to the formation of a weak J-type aggregate, with the molecular transition dipole moments shifted along the molecular axis), there is no clear sign for aggregation.

State Dipole Measurements. From the INDO/SCI calculations obtained from AM1 geometries we extracted the state dipole and the corresponding charge distribution in ground- and excited-state geometries. This information can provide a better insight of the "negative" solvatochromic effect observed experimentally.

Figure 8 pictures the changes in atomic charges when going from the ground state to the lowest electronic excited state of **2** (as calculated at the INDO/SCI level in the ground-state geometry). The corresponding state dipole moments are listed in Table 3. Note that very similar results are obtained when relaxing the geometry in the excited state.

The aniline moiety plays the role of a donor in both the ground and excited state of **2**, which results in the appearance of a dipole pointing with its negative head toward the BODIPY core. However, the INDO/SCI calculations suggest that the ground-state dipole moment in **2** is larger than the excited-state dipole moment so that the dipole moment difference points from the BODIPY to the anilino moiety, see Figure 8. This is responsible for the negative solvatochromic effect observed for this dye: the ground-state absorption spectrum shows a large *blue* shift with increasing solvent polarity (the inertial contribution to the dielectric response stabilizes the ground state to a larger extent than the excited state, hence the blue shift), whereas

a weaker effect is observed in photoluminescence (due to the smaller excited-state dipole). It is interesting to note that this behavior is different from that observed in related BODIPY dyes, such as molecule **3** (Figure 9), in which the amine donor group is separated from the BODIPY core by a styryl spacer. In dye **3**, the charge transfer from the side group to the BODIPY unit is increased upon going from the ground state to the optically allowed electronic excited state. A positive solvatochromic shift is thus predicted and in fact measured[22] for **3**, with a *red* shift of the fluorescence spectrum in high-polarity solvents and a weak dependence of the absorption spectrum on solvent polarizability (electronic part of the dielectric response).

Conclusion

A fluorescent difluoroboron dipyrromethene dye (**2**) with a phenylamino group at the 3-position of the BODIPY core has been synthesized by nucleophilic substitution of 3,5-dichloro-BODIPY (**1**) with aniline. This asymmetrically substituted dye breaks the general symmetry of the BODIPY chromophore. The solvent-dependent photophysical properties have been investigated by means of UV−vis spectrophotometry and steady-state and time-resolved fluorometry. This study demonstrates the large effect of the phenylamino substituent on the fluorescence characteristics of the BODIPY dye. Compound **2** has a low fluorescence quantum yield in most solvents except cyclohexane, toluene, and chloroform. Although its emission maxima [λ_{em}(max)] in a series of solvents from cyclohexane to methanol are red-shifted by approximately 50 nm when compared to typical, symmetric BODIPY derivatives, its absorption maxima wavelengths are not affected by the phenylamino substituent. The $fwhm_{abs}$ and Stokes shifts $\Delta\bar{\nu}$ of BODIPY **2** are much larger than for classic BODIPY derivatives. The values of the fluorescence rate constant of **2** are in the $(1.4-1.7) \times 10^8$ s^{-1} range and do not vary much between the solvents studied. The oxidation potential of **2** in dichloromethane is about 1.14 V versus Ag/AgCl. X-ray analysis shows that the BODIPY core is planar, which is in contrast to the majority of BODIPY compounds found in the CSD database. Moreover, an intramolecular hydrogen bond is observed between the NH group and a fluorine atom. We also performed theoretical simulations of the spectroscopic behavior. Molecular dynamics simulations reveal that there is no clear sign for aggregation of molecule **2** in solution but confirms that the spectral behavior of **2** originates from a negative solvatochromic effect (the inertial contribution to the dielectric response stabilizes the ground state to a larger extent than the excited state).

Acknowledgment. The Belgian IAP-VI/27 program is thanked for continuing support and a fellowship to W.Q. and T.R. The authors are grateful to the Research Council of the K. U. Leuven for Grant GOA 2006/2 and a Junior Fellowship to J.N.C. K.R. thanks the K. U. Leuven for financial support. The Fonds voor Wetenschappelijk Onderzoek−Vlaanderen is thanked for Grant G.0320.00, a predoctoral fellowship to P.D., and a postdoctoral fellowship to K.D. The Instituut voor de aanmoediging van innovatie door Wetenschap en Technologie in Vlaanderen (IWT) is acknowledged for Grant ZWAP 04/007 and for a fellowship to V.L. D.B. is a research associate of the Belgian Fonds National de la Recherche Scientifique (FNRS). B.V.A. thanks the Fonds pour la Recherche en Industrie et en Agriculture (FRIA) for financial support.

Supporting Information Available: Absorption maxima and fluorescence emission maxima for **2** versus $(n^2 - 1)/(2n^2 + 1)$ as a function of solvent, plot of the Stokes shifts of **2** versus the Lippert solvent parameter Δf, and ^{1}H NMR spectrum of **2**. This material is available free of charge via the Internet at http://pubs.acs.org.

References and Notes

(1) Treibs, A.; Kreuzer, F.-H. *Liebigs Ann. Chem.* **1968**, *718*, 208–223.

(2) (a) Ziessel, R.; Ulrich, G.; Harriman, A. *New J. Chem.* **2007**, *31*, 496–501. (b) Loudet, A.; Burgess, K. *Chem. Rev.* **2007**, *107*, 4891–4932. (c) Ulrich, G.; Ziessel, R.; Harriman, A. *Angew. Chem., Int. Ed.* **2008**, *47*, 1184–1201.

(3) (a) Gabe, Y.; Urano, Y.; Kikuchi, K.; Kojima, H.; Nagano, T. *J. Am. Chem. Soc.* **2004**, *126*, 3357–3367. (b) Yamada, K.; Nomura, Y.; Citterio, D.; Iwasawa, N.; Suzuki, K. *J. Am. Chem. Soc.* **2005**, *127*, 6956–6957. (c) Malval, J.-P.; Leray, I.; Valeur, B. *New J. Chem.* **2005**, *29*, 1089–1094. (d) Coskun, A.; Akkaya, E. U. *J. Am. Chem. Soc.* **2005**, *127*, 10464–10465. (e) Wu, Y.; Peng, X.; Guo, B.; Fan, J.; Zhang, Z.; Wang, J.; Cui, A.; Gao, Y. *Org. Biomol. Chem.* **2005**, *3*, 1387–1392. (f) Mei, Y.; Bentley, P. A.; Wang, W. *Tetrahedron Lett.* **2006**, *47*, 2447–2449. (g) Kim, H. J.; Kim, J. S. *Tetrahedron Lett.* **2006**, *47*, 7051–7055. (h) Qi, X.; Jun, E. J.; Xu, L.; Kim, S. J.; Hong, J. S. J.; Yoon, Y. J.; Yoon, J. *J. Org. Chem.* **2006**, *71*, 2881–2884. (i) Yuan, M.; Li, Y.; Li, J.; Li, C.; Liu, X.; Lv, J.; Xu, J.; Liu, H.; Wang, S.; Zhu, D. *Org. Lett.* **2007**, *9*, 2313–2316. (j) Ekmekci, Z.; Yilmaz, M. D.; Akkaya, E. U. *Org. Lett.* **2008**, *10*, 461–464. (k) Namkung, W.; Padmawar, P.; Mills, A. D.; Verkman, A. S. *J. Am. Chem. Soc.* **2008**, *130*, 7794–7795. (l) Yuan, M.; Zhou, W.; Liu, X.; Zhu, M.; Li, J.; Yin, X.; Zheng, H.; Zuo, Z.; Ouyang, C.; Liu, H.; Li, Y.; Zhu, D. *J. Org. Chem.* **2008**, *73*, 5008–5014.

(4) Basarić, N.; Baruah, M.; Qin, W.; Metten, B.; Smet, M.; Dehaen, W.; Boens, N. *Org. Biomol. Chem.* **2005**, *3*, 2755–2761.

(5) (a) Qin, W.; Baruah, M.; De Borggraeve, W. M.; Boens, N. *J. Photochem. Photobiol., A* **2006**, *183*, 190–197. (b) Peng, X.; Du, J.; Fan, J.; Wang, J.; Wu, Y.; Zhao, J.; Sun, S.; Xu, T. *J. Am. Chem. Soc.* **2007**, *129*, 1500–1501.

(6) Baruah, M.; Qin, W.; Vallée, R. A. L.; Beljonne, D.; Rohand, T.; Dehaen, W.; Boens, N. *Org. Lett.* **2005**, *7*, 4377–4380.

(7) Thoresen, L. H.; Kim, H.; Welch, M. B.; Burghart, A.; Burgess, K. *Synlett* **1998**, 1276.

(8) Ulrich, G.; Ziessel, R. *J. Org. Chem.* **2004**, *69*, 2070–2083.

(9) Goud, T. V.; Tutar, A.; Biellmann, J. F. *Tetrahedron* **2006**, *62*, 5084–5091.

(10) (a) Qin, W.; Baruah, M.; Van der Auweraer, M.; De Schryver, F. C.; Boens, N. *J. Phys. Chem. A* **2005**, *109*, 7371–7384. (b) Qin, W.; Baruah, M.; Stefan, A.; Van der Auweraer, M.; Boens, N. *ChemPhysChem* **2005**, *6*, 2343–2351.

(11) Rohand, T.; Baruah, M.; Qin, W.; Boens, N.; Dehaen, W. *Chem. Commun.* **2006**, 266–268.

(12) Rohand, T.; Qin, W.; Boens, N.; Dehaen, W. *Eur. J. Org. Chem.* **2006**, 4658–4663.

(13) Qin, W.; Rohand, T.; Dehaen, W.; Clifford, J. N.; Driessen, K.; Beljonne, D.; Van Averbeke, B.; Van der Auweraer, M.; Boens, N. *J. Phys. Chem. A* **2007**, *111*, 8588–8597.

(14) Rohand, T.; Lycoops, J.; Smout, S.; Braeken, E.; Sliwa, M.; Van der Auweraer, M.; Dehaen, W.; De Borggraeve, W. M.; Boens, N. *Photochem. Photobiol. Sci.* **2007**, *6*, 1061–1066.

(15) (a) Ulrich, G.; Goze, C.; Guardigli, M.; Roda, A.; Ziessel, R. *Angew. Chem., Int. Ed.* **2005**, *44*, 3694–3698. (b) Goze, C.; Ulrich, G.; Mallon, L. J.; Allen, B. D.; Harriman, A.; Ziessel, R. *J. Am. Chem. Soc.* **2006**, *128*, 10231–10239. (c) Goze, C.; Ulrich, G.; Ziessel, R. *J. Org. Chem.* **2007**, *72*, 313–322. (d) Ziessel, R.; Goze, C.; Ulrich, G. *Synthesis* **2007**, 936–949. (e) Tahtaoui, C.; Thomas, C.; Rohmer, F.; Klotz, P.; Duportail, G.; Mély, Y.; Bonnet, D.; Hibert, M. *J. Org. Chem.* **2007**, *72*, 269–272.

(16) (a) López Arbeloa, T.; López Arbeloa, F.; López Arbeloa, I.; García-Moreno, I.; Costela, A.; Sastre, R.; Amat-Guerri, F. *Chem. Phys. Lett.* **1999**, *299*, 315–321. (b) Costela, A.; García-Moreno, I.; Gomez, C.; Sastre, R.; Amat-Guerri, F.; Liras, M.; López Arbeloa, F.; Bañuelos Prieto, J.; López Arbeloa, I. *J. Phys. Chem. A* **2002**, *106*, 7736–7742. (c) López Arbeloa, F.; Bañuelos Prieto, J.; Martínez Martínez, V.; Arbeloa López, T.; López Arbeloa, I. *ChemPhysChem* **2004**, *5*, 1762–1771. (d) Bañuelos Prieto, J.; López Arbeloa, F.; Martínez Martínez, V.; Arbeloa López, T.; Amat-Guerri, F.; Liras, M.; López Arbeloa, I. *Chem. Phys. Lett.* **2004**, *385*, 29–35.

(17) Kollmannsberger, M.; Rurack, K.; Resch-Genger, U.; Daub, J. *J. Phys. Chem. A* **1998**, *102*, 10211–10220.

(18) Baruah, M.; Qin, W.; Flors, C.; Hofkens, J.; Vallée, R. A. L.; Beljonne, D.; Van der Auweraer, M.; De Borggraeve, W. M.; Boens, N. *J. Phys. Chem. A* **2006**, *110*, 5998–6009.

(19) Baruah, M.; Qin, W.; Basarić, N.; De Borggraeve, W. M.; Boens, N. *J. Org. Chem.* **2005**, *70*, 4152–4157.

(20) Qin, W.; Rohand, T.; Baruah, M.; Stefan, A.; Van der Auweraer, M.; Dehaen, W.; Boens, N. *Chem. Phys. Lett.* **2006**, *420*, 562–568.

(21) (a) Rurack, K.; Kollmannsberger, M.; Daub, J. *New J. Chem.* **2001**, *25*, 289–292. (b) Rurack, K.; Kollmannsberger, M.; Daub, J. *Angew. Chem., Int. Ed.* **2001**, *40*, 385–387. (c) Coskun, A.; Deniz, E.; Akkaya, E. U. *Org. Lett.* **2005**, *7*, 5187–5189.

(22) Qin, W.; Baruah, M.; Sliwa, M.; Van der Auweraer, M.; De Borggraeve, W. M.; Beljonne, D.; Van Averbeke, B.; Boens, N. *J. Phys. Chem. A* **2008**, *112*, 6104–6114.

(23) Sheldrick, G. M. SHELXL97; University of Göttingen: Göttingen, Germany, 1997.

(24) Olmsted, J. *J. Phys. Chem.* **1979**, *83*, 2581–2584.

(25) Valeur, B. *Molecular Fluorescence. Principles and Applications*; Wiley-VCH: Weinheim, Germany, 2002.

(26) (a) O'Connor, D. V.; Phillips, D. *Time-Correlated Single Photon Counting*; Academic Press: New York, 1984. (b) vandeVen, M.; Ameloot, M.; Valeur, B.; Boens, N. *J. Fluoresc.* **2005**, *15*, 377–413. (c) Boens, N.; Qin, W.; Basarić, N.; Hofkens, J.; Ameloot, M.; Pouget, J.; Lefèvre, J.-P.; Valeur, B.; Gratton, E.; vandeVen, M.; Silva, N. D.; Engelborghs, Y.; Willaert, K.; Sillen, A.; Rumbles, G.; Phillips, D.; Visser, A. J. W. G.; Van Hoek, A.; Lakowicz, J. R.; Malak, H.; Gryczynski, I.; Szabo, A. G.; Krajcarski, D. T.; Tamai, N.; Miura, A. *Anal. Chem.* **2007**, *79*, 2137–2149.

(27) Crovetto, L.; Orte, A.; Talavera, E. M.; Alvarez-Pez, J. M.; Cotlet, M.; Thielemans, J.; De Schryver, F. C.; N. Boens, N. *J. Phys. Chem. B* **2004**, *108*, 6082–6092.

(28) Van den Zegel, M.; Boens, N.; Daems, D.; De Schryver, F. C. *Chem. Phys.* **1986**, *101*, 311–335.

(29) Dewar, M. J. S.; Zoebisch, E. G.; Healy, E. F.; Stewart, J. J. P. *J. Am. Chem. Soc.* **1985**, *107*, 3902–3909.

(30) Becke, A. D. *J. Chem. Phys.* **1993**, *98*, 1372–1377.

(31) Zerner, M. C. In *Reviews in Computational Chemistry*; Lipkowitz, K. W., Boyd, D. B., Eds.; VCH: New York, 1991; Vol. 2, pp 313−365.

(32) Mayo, S. L.; Olafson, B. D.; Goddard, W. A., III. *J. Phys. Chem.* **1990**, *94*, 8897–8909.

(33) Allen, F. H. *Acta Crystallogr.* **2002**, *B58*, 380–388.

(34) Vos de Wael, E.; Pardoen, J. A.; van Koeveringe, J. A.; Lugtenburg, J. *Recl. Trav. Chim. Pays-Bas* **1977**, *96*, 306–309.

(35) (a) Marcus, R. A. *J. Chem. Phys.* **1965**, *43*, 1261–1265. (b) Brunschwig, S.; Ehrenson, S.; Sutin, N. *J. Phys. Chem.* **1987**, *91*, 4714–4722. (c) Verbeek, G.; Depaemelaere, S.; Van der Auweraer, M.; De Schryver, F. C.; Vaes, A.; Terrell, D.; De Meutter, S. *Chem. Phys.* **1993**, *176*, 195–213.

(36) (a) Brooker, L.G. S.; Keyes, G. H.; Williams, W. *J. Am. Chem. Soc.* **1942**, *64*, 199–210. (b) Brooker, L.G. S.; Keyes, G. H.; Sprague, R. H.; Van Dyke, R. H.; Van Lare, E.; Van Zandt, G.; White, F. L.; Cressman, H. W. J.; Dent, S. G. *J. Am. Chem. Soc.* **1951**, *73*, 5332–5350.

(37) Lippert, E. *Z. Naturforsch., A: Phys. Sci.* **1955**, *10*, 541–545.

(38) Mataga, N.; Kaifu, Y.; Koizumi, M. *Bull. Chem. Soc. Jpn.* **1955**, *28*, 690−691; **1956**, *29*, 465−470.

(39) (a) Bergström, F.; Mikhalyov, I.; Hägglöf, P.; Wortmann, R.; Ny, T.; Johansson, L. B.-Å. *J. Am. Chem. Soc.* **2002**, *124*, 196–204. (b) Mikhalyov, I.; Gretskaya, N.; Bergström, F.; Johansson, L. B. *Phys. Chem. Chem. Phys.* **2002**, *4*, 5663–5670. (c) Tleugabulova, D.; Zhang, Z.; Brennan, J. D. *J. Phys. Chem. B* **2002**, *106*, 13133–13138.

JP8077584